Electronic Supplementary Material (ESI) for Environmental Science: Processes & Impacts.

Electronic Supplementary Information for

Mandelic Acid and Phenyllactic Acid "Reaction Sets" for Exploring the Kinetics and Mechanism of Oxidations by Hydrous Manganese Oxide (HMO)

*Xiaomeng Xia and Alan T. Stone**

Department of Environmental Health and Engineering

Whiting School of Engineering

Johns Hopkins University

Baltimore, MD 21218

(*Corresponding author: astone@jhu.edu, Tel.: 410-516-8476)

S1: Environmental Significance of α-Hydroxycarboxylic Acids, α-Ketocarboxylic Acids, and Aldehydes

Glycolic acid, lactic acid, and malic acid (Figure S1) are the three most commonly used α-hydroxycarboxylic acids in dermatological pharmaceuticals (applied topically) and over-the-counter skin care products, where they can represent 2 to 70 % of the product by weight.[1, 2]

Pyruvic acid is commonly used in skin peel formulations. Pyruvic acid, along with the aliphatic α-ketocarboxylic acids oxaloacetic acid and α-hydroxyglutaric acid (Figure S2) are important intermediates in biochemical cycles.

Owing to the complexity of natural organic matter (NOM) molecular structures, researchers frequently include low molecular-weight surrogate compounds in their investigations of chemical reactions that lead to the formation of disinfection by-products. Figure S3 lists illustrative α-hydroxycarboxylic acids, α-ketocarboxylic acids, and aldehydes that Bond *et al.*[3] compiled in a survey of surrogates for the production of trihalomethanes and haloacetic acids.[4-7] Aliphatic aldehydes and benzaldehydes are commonly reported products of natural organic matter oxidation by ozone.[8-10]

Within soils, Mn^{II} generated within O_2-poor, organic matter-rich reducing microzones diffuses outward until the O_2 concentrations are high enough for re-oxidation by manganese oxidizing bacteria.[11] Any organic compounds diffusing across redox gradients may be subject to oxidation by manganese oxyhydroxides.

Lignin, the second most abundant terrestrial biopolymer,[12] is the product of the biologically-regulated radical coupling of three compounds possessing the styrene moiety: coumaryl alcohol, coniferyl alcohol, and sinapyl alcohol. Conceptualizations of lignin structures

and surrogate compounds used to explore lignin chemistry (e.g. Ragnar et al.,[13] Pollegioni *et al.*[14]) are included in Figure S4. β-O-4 linkages where oxygens are found at positions both α- and β-carbons relative to benzene rings[15] are relatively easily transformed via chemical reaction to the α-hydroxycarboxylic acids under investigation in our own study. Fungal decomposition of lignin generates methoxy-, hydroxy-substituted mandelic acids,[16] and substituted phenylglyoxylic acids, phenylpyruvic acids, and aromatic aldehydes are commonly generated from lignin during industrial chemical processes that are part of pulp and paper manufacture.[17, 18] The aromatic portion of soil organic matter is believed to be largely derived from lignin breakdown products.

Degradation products of two plant polyesters, suberin and cutin,[19] are believed to be important contributors to the aliphatic portion of soil organic matter.[20] 2-Hydroxytetracosanoic acid (Figure S5) is believed to be refractory enough to serve as a biomarker.[20] Manganese oxyhydroxides in soils are capable of oxidizing them, their utility as biomarkers would be somewhat restricted.

Soil organisms exude a wide range of biochemicals for fulfilling specific functions. If these compounds are degraded by manganese oxyhydroxides, their biological utility is lost. Figure S6 provides three illustrative examples. Mugineic acid is one of approximately seven phytosiderphores that have been described, which grasses exude as siderophores for the acquisition of Fe^{III}.[21] Corrugatin is an example of a bacterial siderophore that possesses two α-hydroxycarboxylic acid groups alongside other Fe^{III}-coordinating Lewis base groups. Corrugatin is produced by the plant pathogen *Pseudomonas corrugata* found in soils.[22] Piscidic acid is exuded by the roots of pigeon pea (*Cajanus cajan*), a legume crop. It solubilizes adsorbed

orthophosphate within soils by bringing about the ligand-assisted dissolution of the Fe^{III} and Al^{III} oxyhydroxide sorbent phases.[23]

Manganese within atmospheric aerosols is present in the nM to tens of nM range.[24] While Mn^{II} predominates during sunlit hours, particulate Mn^{III} (and Mn^{IV}) is believed in increase at night.[25] Mn and Cu are the two most important transition metals with regards to redox processes taking place within atmospheric aerosols.[26, 27]

α-Hydroxycarboxylic acids, α-ketocarboxylic acids, and aldehydes are important functional groups of organic compounds within atmospheric aerosols (Figure S7).[28, 29] All are believed to arise from the photooxidation of volatile biological alkenes, the most important being isoprene.[30] 2-Hydroxy-4-isopropyladipic acid is an early intermediate in isoprene photooxidation, while pyruvic acid and malic acid are more fully oxidized products.[28, 29, 31] 2-Ketooctanoic acid is an illustrative example of an ionized compound found in atmospheric aerosols ultimately derived from marine phytoplankton-biosynthesized long-chain alkenes.[32] Owing to their hygroscopicity, the compounds shown in Figure S7 are in part responsible for the ability of atmospheric aerosols to serve as cloud condensation nuclei.[29, 33, 34]

S2: Calculation of the Expected Reaction Stoichiometry for the Formation of Mn^{II}

Three half reactions can be derived from Figure 2.1 for expressing stoichiometries of hydroxy acid oxidation to keto acid, aldehyde, and C-1 acid:

$$RCH(OH)COO^- = R(CO)COO^- + 2H^+ + 2e^- \quad \text{(S1)}$$

$$RCH(OH)COO^- + H_2O = R(CO)H + H_2CO_3^* + H^+ + 2e^- \quad \text{(S2)}$$

$$RCH(OH)COO^- + 2H_2O = RCOOH + H_2CO_3^* + 3H^+ + 4e^- \quad \text{(S3)}$$

For the sake of completeness, half reactions for oxidation of keto acid and aldehyde to C-1 acid are shown below:

$$R(CO)COO^- + 2H_2O = RCOOH + H_2CO_3^* + H^+ + 2e^- \quad (S4)$$

$$R(CO)H + H_2O = RCOOH + 2H^+ + 2e^- \quad (S5)$$

As noted in Section 2.3.2, iodometric titration of two of the HMO suspensions employed in our experiments yielded an average manganese oxidation state of +3.82. Oxygen atoms within oxyhydroxide minerals exist in the -II oxidation state. HMO can accordingly be represented as $MnO_{1.91}(s)$, and the half reaction for generating Mn^{II} becomes:

$$MnO_{1.91}(s) + 3.82H^+ + 1.82e^- = Mn^{II} + 1.91H_2O \quad (S6)$$

S1, S2, S4, and S6 are two-electron steps oxidations. In order to add Reaction S6 to organic half reactions obtain balanced full reactions, it must be multiplied by 1.10:

$$1.10MnO_{1.91}(s) + 4.20H^+ + 2e^- = 1.10Mn^{II} + 2.10H_2O \quad (S7)$$

S3 is a four-electron oxidation, hence Reaction S6 must be multiplied by 2.20:

$$2.20MnO_{1.91}(s) + 8.40H^+ + 4e^- = 2.20Mn^{II} + 4.20H_2O \quad (S8)$$

Summing appropriate half reactions yields five full equations:

Hydroxy Acid Oxidation to Keto Acid (S1 + S7)

$$1.10MnO_{1.91}(s) + 4.20H^+ + 2e^- = 1.10Mn^{II} + 2.10H_2O$$

$$\underline{RCH(OH)COO^- = R(CO)COO^- + 2H^+ + 2e^-}$$

add: $RCH(OH)COO^- + 1.10MnO_{1.91}(s) + 2.20H^+ = R(CO)COO^- + 1.10Mn^{II} + + 2.10H_2O$ (S9)

Hydroxy Acid Oxidation to Aldehyde (S2 + S7)

$$1.10MnO_{1.91}(s) + 4.20H^+ + 2e^- = 1.10Mn^{II} + 2.10H_2O$$

$$\underline{RCH(OH)COO^- + H_2O = R(CO)H + H_2CO_3^* + H^+ + 2e^-}$$

add: $RCH(OH)COO^- + 1.10MnO_{1.91}(s) + 3.20H^+ = R(CO)H + H_2CO_3^* + 1.10Mn^{II} + 1.10H_2O$ (S10)

Hydroxy Acid Oxidation to C-1 Acid (S3 + S8)

$$2.20MnO_{1.91}(s) + 8.40H^+ + 4e^- = 2.20Mn^{II} + 4.20H_2O$$

$$\underline{RCH(OH)COO^- + 2H_2O = RCOOH + H_2CO_3^* + 3H^+ + 4e^-}$$

add: $RCH(OH)COO^- + 2.20MnO_{1.91}(s) + 5.40H^+ = RCOOH + H_2CO_3^* + 2.20Mn^{II} + 2.20H_2O$ (S11)

Keto Acid Oxidation to C-1 Acid (S4 + S7)

$$1.10MnO_{1.91}(s) + 4.20H^+ + 2e^- = 1.10Mn^{II} + 2.10H_2O$$

$$\underline{R(CO)COO^- + 2H_2O = RCOOH + H_2CO_3^* + H^+ + 2e^-}$$

add: $R(CO)COO^- + 1.10MnO_{1.91}(s) + 3.20H^+ = RCOOH + H_2CO_3^* + 1.10Mn^{II} + 0.10H_2O$ (S12)

Aldehyde Oxidation to C-1 Acid (S5 + S7)

$$1.10MnO_{1.91}(s) + 4.20H^+ + 2e^- = 1.10Mn^{II} + 2.10H_2O$$

$$\underline{R(CO)H + H_2O = RCOOH + 2H^+ + 2e^-}$$

add: $R(CO)H + 1.10MnO_{1.91}(s) + 2.20H^+ = RCOOH + 1.10Mn^{II} + 1.10H_2O$ (S13)

In experiments where reaction set organic compounds do not adsorb to a significant extent and mass balance is obeyed (i.e. the sum of concentrations of reaction set compounds equals the concentration of organic substrate added), Equations S9-S13 can be used to calculate expected amounts of Mn^{II} generated.

S3: Equilibrium Speciation of Reaction Set Compounds

In this section we present the available equilibrium data for the eight organic compounds that comprise our two reaction sets. For speciation calculations at pH 4.0, the medium was defined using 5.0 mM acetate and 10 mM NaCl, which fixes the ionic strength at 15 mM. For comparison purposes, speciation calculations at pH 7.0 also assumed that the ionic strength was fixed at 15 mM. At this ionic strength, the Davies Equation can be used to calculate $\gamma_{\pm} = 0.8865$ and $\gamma_{2\pm} = 0.6177$.

Mandelic Acid

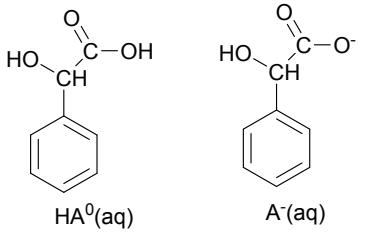

$HA^0(aq)$ $A^-(aq)$

$HA^0(aq) = A^-(aq) + H^+(aq)$ $\quad {}^aK_a = 10^{-3.40\ 35}$

$${}^aK_a = \frac{\{A^-(aq)H^+(aq)\}}{\{HA^0(aq)\}} = \gamma_{\pm}\gamma_{\pm}{}^cK_a \qquad {}^cK_a = \frac{[A^-(aq)][H^+(aq)]}{[HA^0(aq)]} = 10^{-3.30}$$

At $p^aH = 4.0$, $p^cH = 3.948$. At $p^aH = 7.0$, $p^cH = 6.948$.

$A_T = [HA^0(aq)] + [A^-(aq)]$

		At $p^aH = 4.0$	At $p^aH = 7.0$
Algebra yields:	$\frac{[HA^0(aq)]}{A_T} = \frac{[H^+(aq)]}{[H^+(aq)] + {}^cK_a}$	0.182	2.22×10^{-4}
	$\frac{[A^-(aq)]}{A_T} = \frac{{}^cK_a}{[H^+(aq)] + {}^cK_a}$	0.818	0.9998

Phenylglyoxylic Acid = Benzoylformic Acid

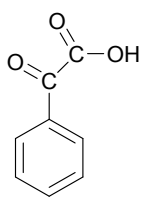

$HW^0(aq)$

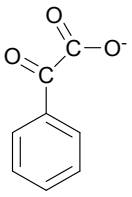

$W^-(aq)$

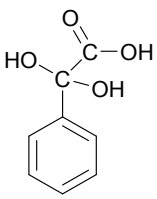

$HX^0(aq)$

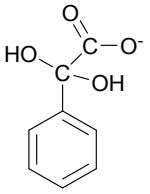

$X^-(aq)$

$HW^0(aq) = W^-(aq) + H^+(aq)$ $\quad {}^aK_a = 10^{-2.05\ 36}$

$$ {}^cK_a = 10^{-1.95} = \frac{[L^-(aq)][H^+(aq)]}{[HL^0(aq)]} $$

Lopalco et al. (2016)[32] state that for the reaction $W^-(aq) = X^-(aq)$, $K_H(ion) < 10^{-3}$.

Let's assume that $HX^0(aq)$ can be ignored in the range $4 < pH < 7$.

$W_T = [HW^0] + [W^-] + [X^-] = ([H^+]/{}^cK_a + 1 + K_H(ion))[W^-]$

		At $p^aH = 4.0$	At $p^aH = 7.0$
Algebra yields:	$[HW^0]/W_T$	9.94×10^{-3}	1.00×10^{-5}
	$[W^-]/W_T$	0.989	0.999
	$[X^-]/W_T$	9.89×10^{-4}	9.99×10^{-4}

At pH 4, the ketocarboxylate anion form HX^0 is predominant, with much lower concentrations of the conjugate keto acid form HW^0 (1/100) and the anionic, hydrate form X^- (< 1/1000). At pH 7, the ketocarboxylate anion is still predominant, but the conjugate acid keto form concentration is much lower (< 1/10,000). The amount of anionic, hydrate form remains the same (< 1/1000).

Benzaldehyde

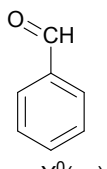

$Y^0(aq)$

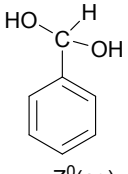

$Z^0(aq)$

At neutral and acidic pHs, the hydrated form is approximately 0.8 % of total benzaldehyde.[37, 38]

Benzoic Acid

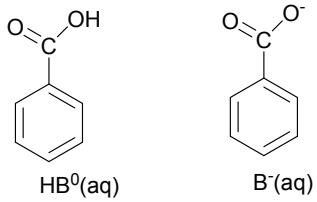

$HB^0(aq)$ $B^-(aq)$

$HB^0(aq) = B^-(aq) + H^+(aq)$ $\quad {}^aK_a = 10^{-4.202}$ [35]

${}^cK_a = 10^{-4.097}$

		At $p^aH = 4.0$	At $p^aH = 7.0$
Algebra yields:	$\frac{[HB^0(aq)]}{B_T} = \frac{[H^+(aq)]}{[H^+(aq)] + {}^cK_a}$	0.585	1.41×10^{-3}
	$\frac{[B^-(aq)]}{B_T} = \frac{{}^cK_a}{[H^+(aq)] + {}^cK_a}$	0.415	0.9986

Phenyllactic Acid

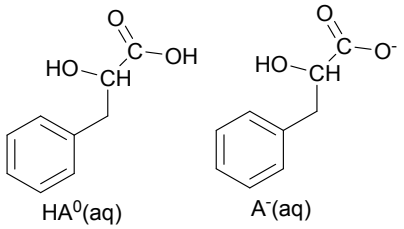

$HA^0(aq)$ $A^-(aq)$

We have not found a reliable pK_a for phenyllactic acid in the literature.

Phenylpyruvic Acid

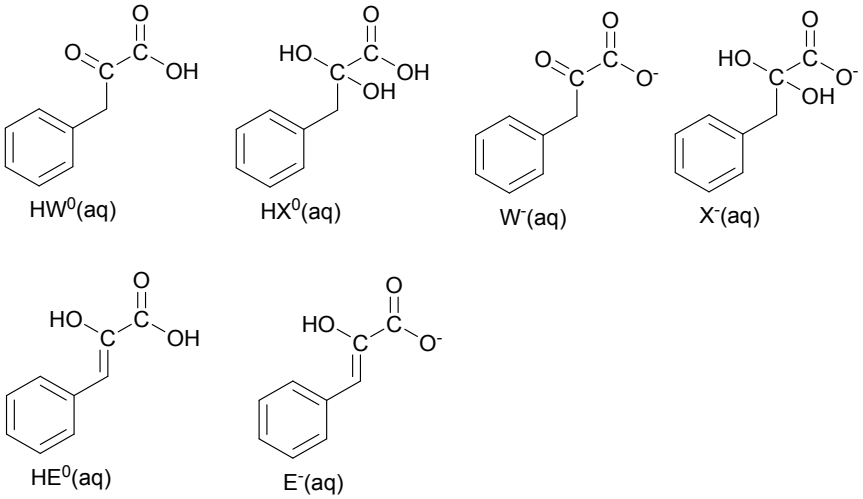

We have not found reliable thermodynamic data for phenylpyruvic acid. If we assume that speciation is similar to that of pyruvic acid, we have the following data from Chiang et al.,[39] which has been subsequently cited by Kerber and Fernando[40] and Galajda et al.:[41]

$HW^0(aq) = W^-(aq) + H^+(aq)$ $10^{-1.97}$

$HW^0(aq) = HX^0(aq)$ $10^{+0.36}$

$HW^0(aq) = HE^0(aq)$ $10^{-3.21}$

$HX^0(aq) = X^-(aq) + H^+(aq)$ $10^{-3.53}$

$HE^0(aq) = E^-(aq) + H^+(aq)$ $10^{-3.79}$

$E^-(aq) = H_{-1}E^{2-}(aq) + H^+(aq)$ $10^{-11.55}$

The ionic strength that these constants correspond to has not be clearly stated in the three papers cited. Hence, even for pyruvic acid, we have to treat any calculations as provisional.

	$\frac{[i]}{L_T}$	
	p^aH 4.00	p^aH 7.00
$W^-(aq)$	0.914	0.941
$X^-(aq)$	5.77×10^{-2}	5.93×10^{-2}
$HX^o(aq)$	1.95×10^{-2}	2.11×10^{-5}

$HY^{o}(aq)$	$9.32x10^{-3}$	$8.78x10^{-6}$
$E^{-}(aq)$	$8.53x10^{-6}$	$8.78x10^{-6}$
$HE^{o}(aq)$	$5.26x10^{-6}$	$5.41x10^{-9}$
$H_{-1}E^{2-}(aq)$	$2.58x10^{-13}$	$2.65x10^{-10}$

At pH 4.0, the two hydrated forms represent 7.7 % of the total concentration. Only one molecule in 73,000 is in the enol form (Figure S16).

Phenylacetaldehyde

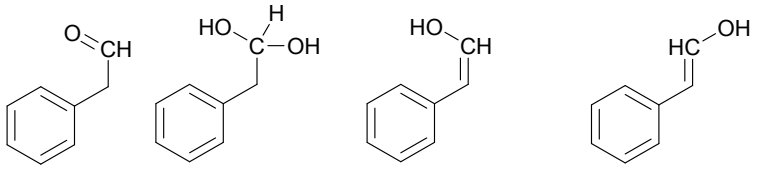

$Y^{0}(aq)$ $Z^{0}(aq)$ $cF^{o}(aq)$ = *cis*-enol $tF^{o}(aq)$ = *trans*-enol

Chiang et al.[42] have presented the following thermodynamic information:

$$Y^{o}(aq) + H_2O(l) = Z^{o}(aq) \quad K_1 = 2.93 = \frac{[Z^{o}(aq)]}{[Y^{o}(aq)]}$$

$$Y^{o}(aq) = cF^{o}(aq) \quad K_2 = 10^{-3.35} = \frac{[cF^{o}(aq)]}{[Y^{o}(aq)]}$$

$$Y^{o}(aq) = tF^{o}(aq) \quad K_3 = 10^{-3.07} = \frac{[tF^{o}(aq)]}{[Y^{o}(aq)]}$$

Since all these species mentioned above are electrically neutral, there are no ionic strength effects to consider. Also, they all exist at the same protonation level, so their relative equilibrium abundance is not a function of pH.

$$P_T = [Y^{o}(aq)] + [Z^{o}(aq)] + [cF^{o}(aq)] + [tF^{o}(aq)] = [Y^{o}(aq)](1 + 2.93 + 4.47x10^{-4} + 8.51x10^{-4})$$

We obtain: $[Y^{o}(aq)]/P_T = 0.254$ $[cF^{o}(aq)]/P_T = 1.35x10^{-4}$

$[Z^{o}(aq)]/P_T = 0.745$ $[tF^{o}(aq)]/P_T = 2.16x10^{-4}$

Here, the hydrated form represents 75 % of the total concentration. Only one molecule in 2850 exists as one of the two enol forms.

Phenylacetic Acid

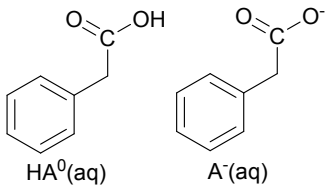

$HA^0(aq)$ $A^-(aq)$

$HA^0(aq) = A^-(aq) + H^+(aq)$ $\quad {}^aK_a = 10^{-4.310\ 35}$ $\quad {}^cK_a = 10^{-4.205}$

		At $p^aH = 4.0$	At $p^aH = 7.0$
$\frac{[HA^0(aq)]}{A_T}$ =	$\frac{[H^+(aq)]}{[H^+(aq)] + {}^cK_a}$	0.644	1.80×10^{-3}
$\frac{[A^-(aq)]}{A_T}$ =	$\frac{{}^cK_a}{[H^+(aq)] + {}^cK_a}$	0.356	0.998

Table S1. Hydrous manganese oxide (HMO) preparations employed in the experiments.

Designation	Date Synthesized	Mn Loading (mM)	Average Mn Oxidation State (Days)
HMO-A	2014-3-26	5.0	-
HMO-B	2014-5-12	5.2	+3.82 ± 0.02 (2*)
HMO-C	2014-6-13	5.0	+3.82 ± 0.03 (3*, 10*)
HMO-D	2014-8-15	5.4	-
HMO-E	2014-10-3	5.1	-
HMO-F	2015-2-10	5.0	-
HMO-G	2016-7-12	5.0	-
HMO-H	2016-6-6	5.1	-

*Age of HMO when tested

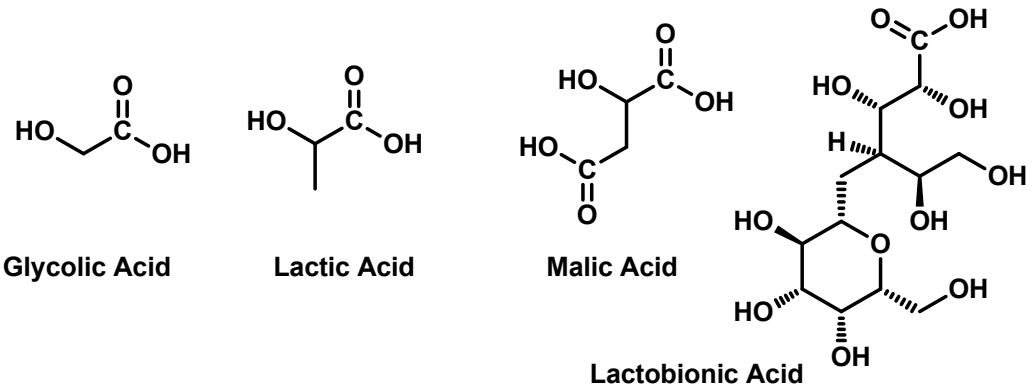

Figure S1. The α-hydroxycarboxylic acids glycolic acid, lactic acid, and malic acid are heavily employed in dermatological pharmaceuticals (applied topically) and over-the-counter skin care formulations. Lactobionic acid is also common in skin formulations. Hydroxyl groups both α- and β- to the carboxylic acid group are important for its pharmacological properties and its chemical reactivity.

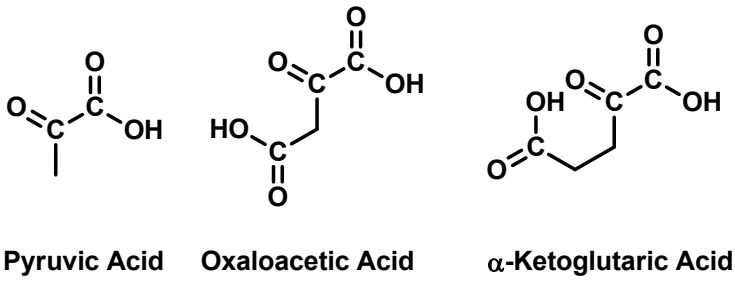

Figure S2. Pyruvic acid is a common ingredient in skin peeling formulations. Oxaloacetic acid and α-ketoglutaric acid are important in biochemical cycles, but have found little if any commercial application.

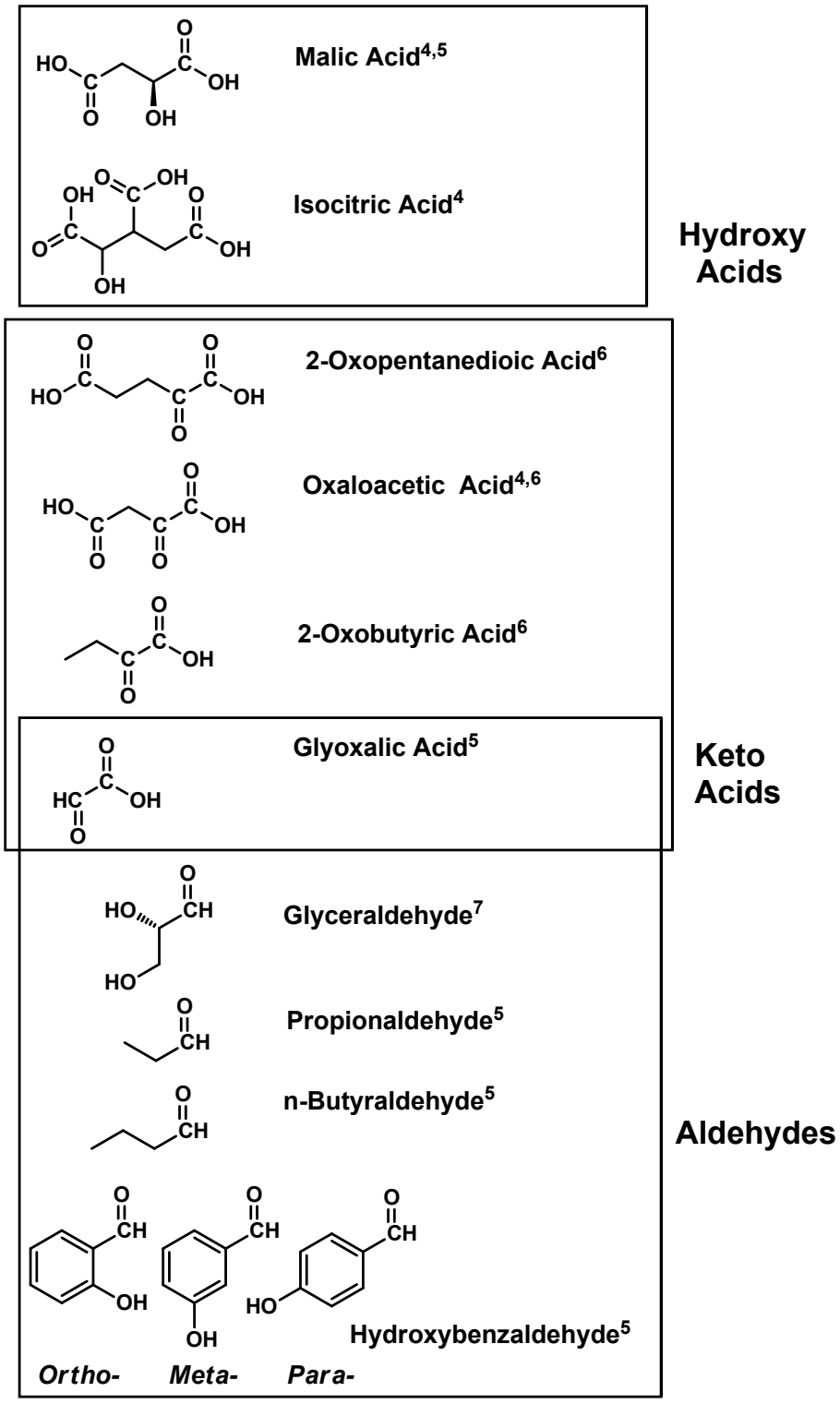

Figure S3. Hydroxy acid, keto acid, and aldehyde natural organic matter surrogates (i.e. disinfection byproduct precursors) used in studies of drinking water disinfection studies, as compiled by Bond *et al.*[3]

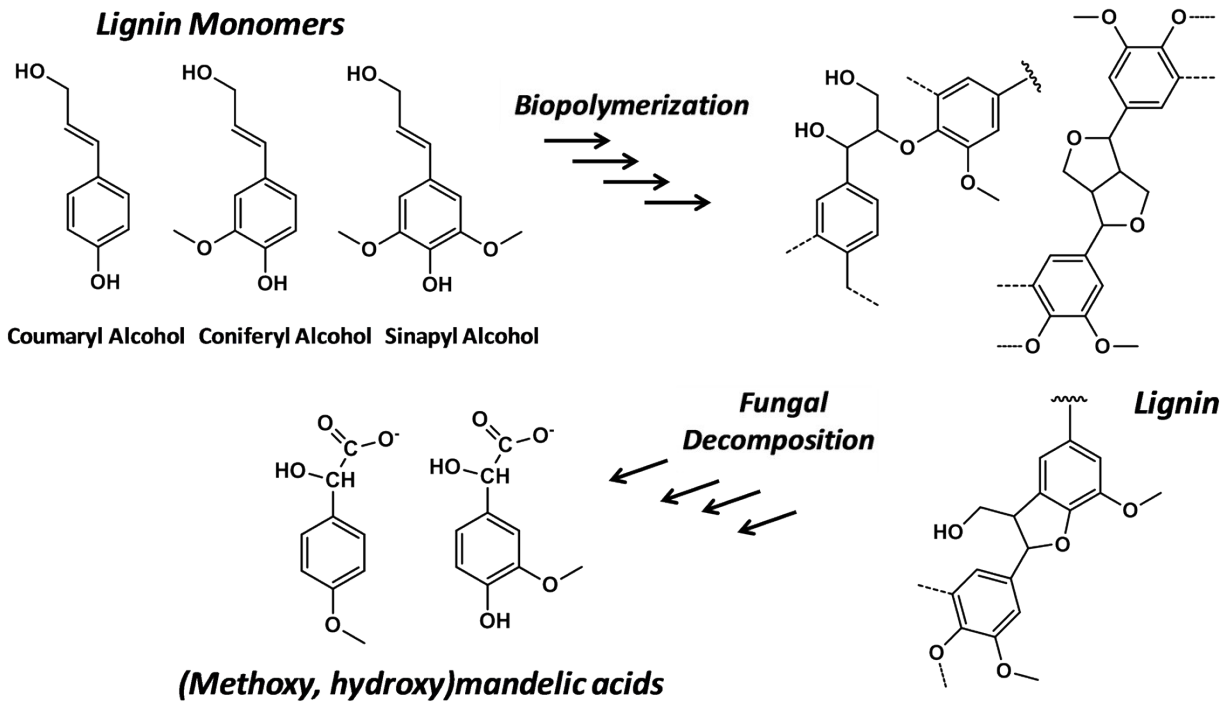

Figure S4. As mentioned in the main text, any time styrene moieties are oxidized, products include mandelic acid- and phenyllactic acid-like structures. Lignin is the product of the controlled radical oxidation of coumaryl alcohol, coniferal alcohol, and sinapyl alcohol, yielding aromatic-aromatic linkages depicted to the right of the figure.[13-15] Fungal decomposition of lignin can yield methoxy- and hydroxy-substituted mandelic acids depicted at the bottom left of the figure.[16]

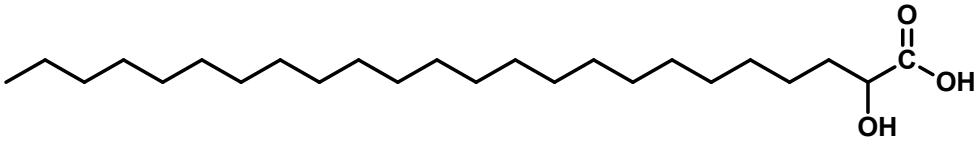

Figure S5. 2-Hydroxytetracosanoic acid is a biomarker in soil organic matter, reflecting inputs of the biopolymers cutin and suberin.

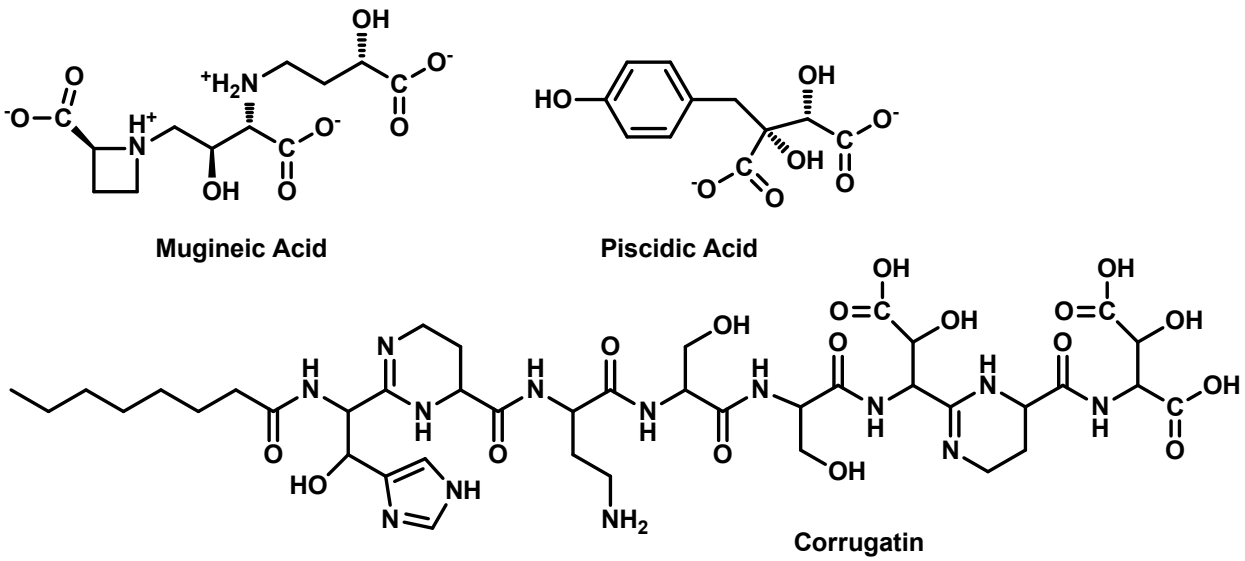

Figure S6. Biological soil exudates bearing α-hydroxycarboxylic acid moieties. Mugineic acid is a siderophore first identified in the rhizosphere of barley.[21] Corrugatin is a siderophore produced by the plant pathogen *Pseudomonas corrugata*.[22] Piscidic acid is not strictly a siderophore, since it has not been reported to increase iron uptake. It is believed to bring about the ligand-assisted dissolution of soil Fe^{III} and Al^{III} oxyhydroxides, and in the process release the plant nutrient orthophosphate.[23]

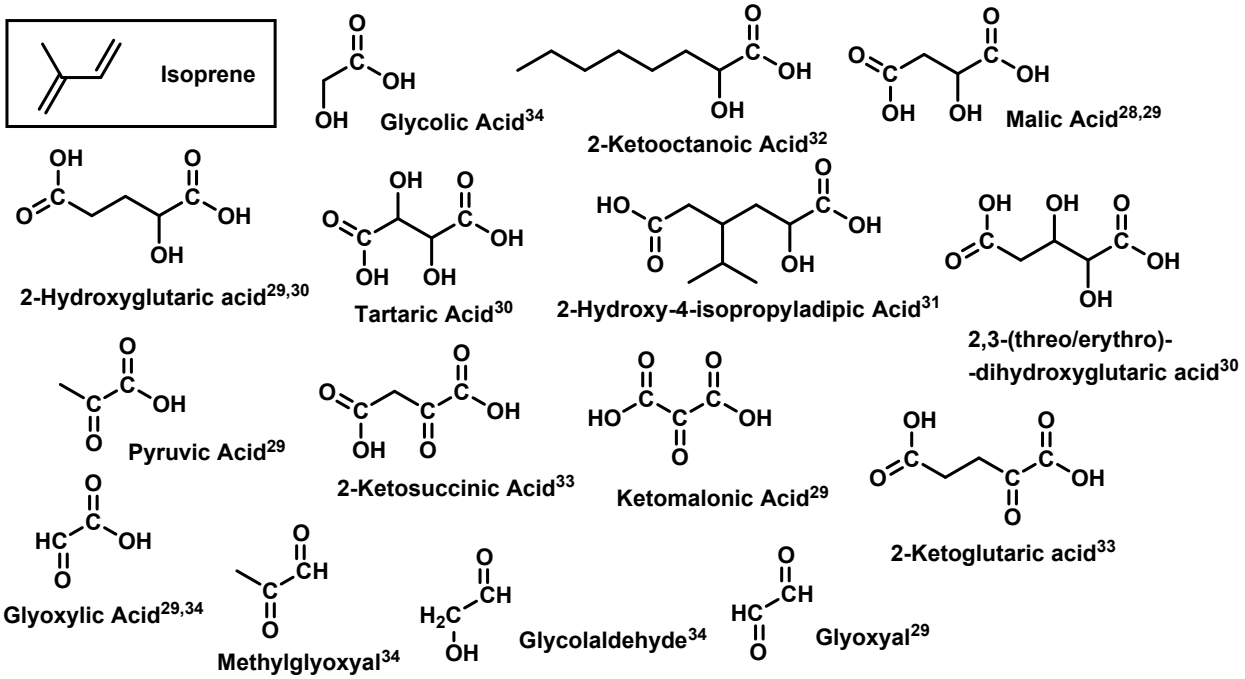

Figure S7. α-Hydroxycarboxylic acids, α-ketocarboxylic acids, aldehydes, and compounds bearing multiple groups that have been identified in atmospheric aerosols. They are created via photooxidation of biological alkenes. Isoprene is believed to be the most important alkene precursor compound.

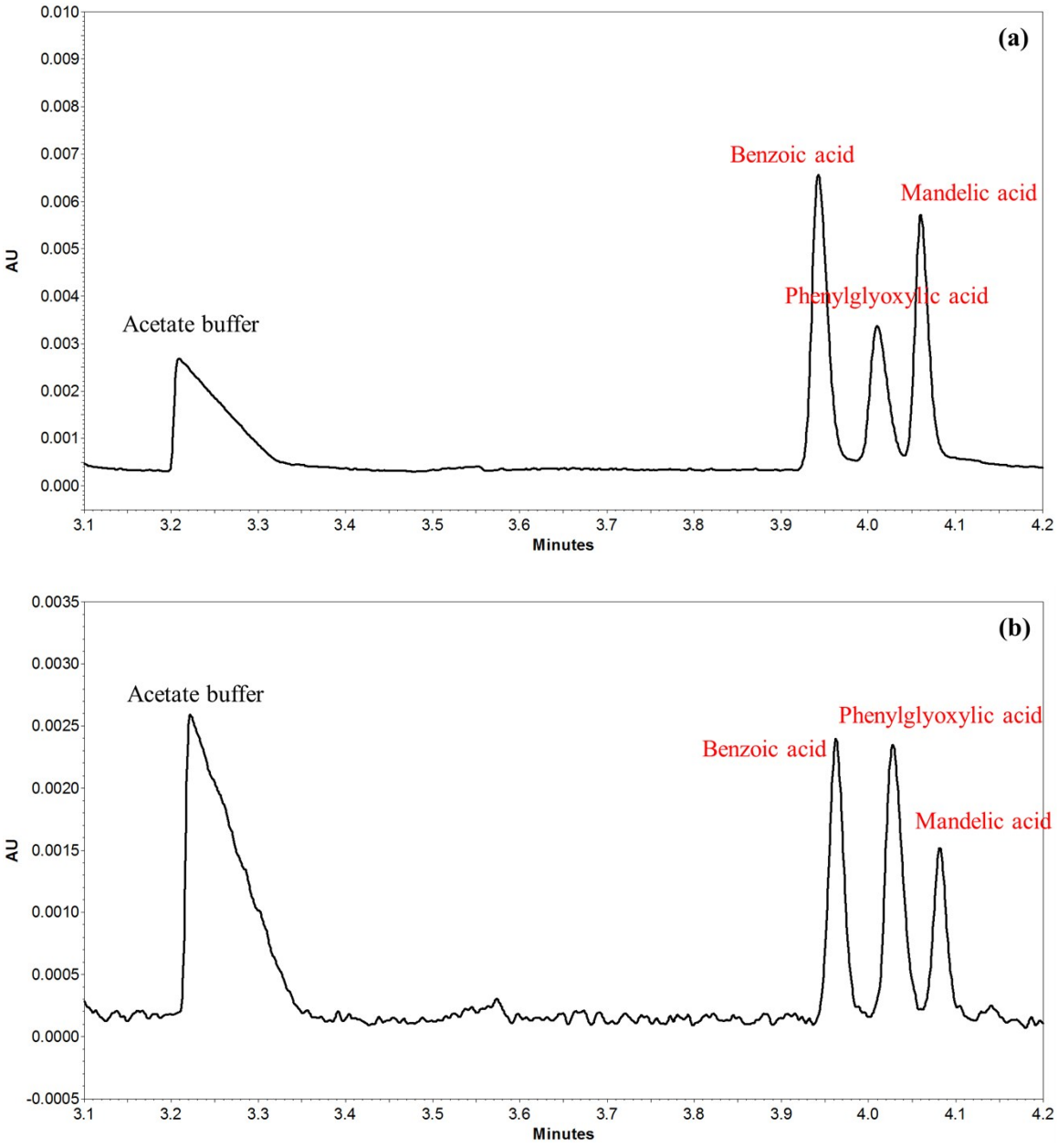

Figure S8. Illustrative electropherogram of (a) authentic organic substrates standard solution (20 µM benzoic acid, 10 µM phenylglyoxylic acid, and 20 µM mandelic acid) and (b) filtered reaction solution collected 6 hours after addition of 500 M HMO to 50 µM mandelic acid. All solutions contain 5 mM acetate buffer (pH 4.0) and 10 mM NaCl.

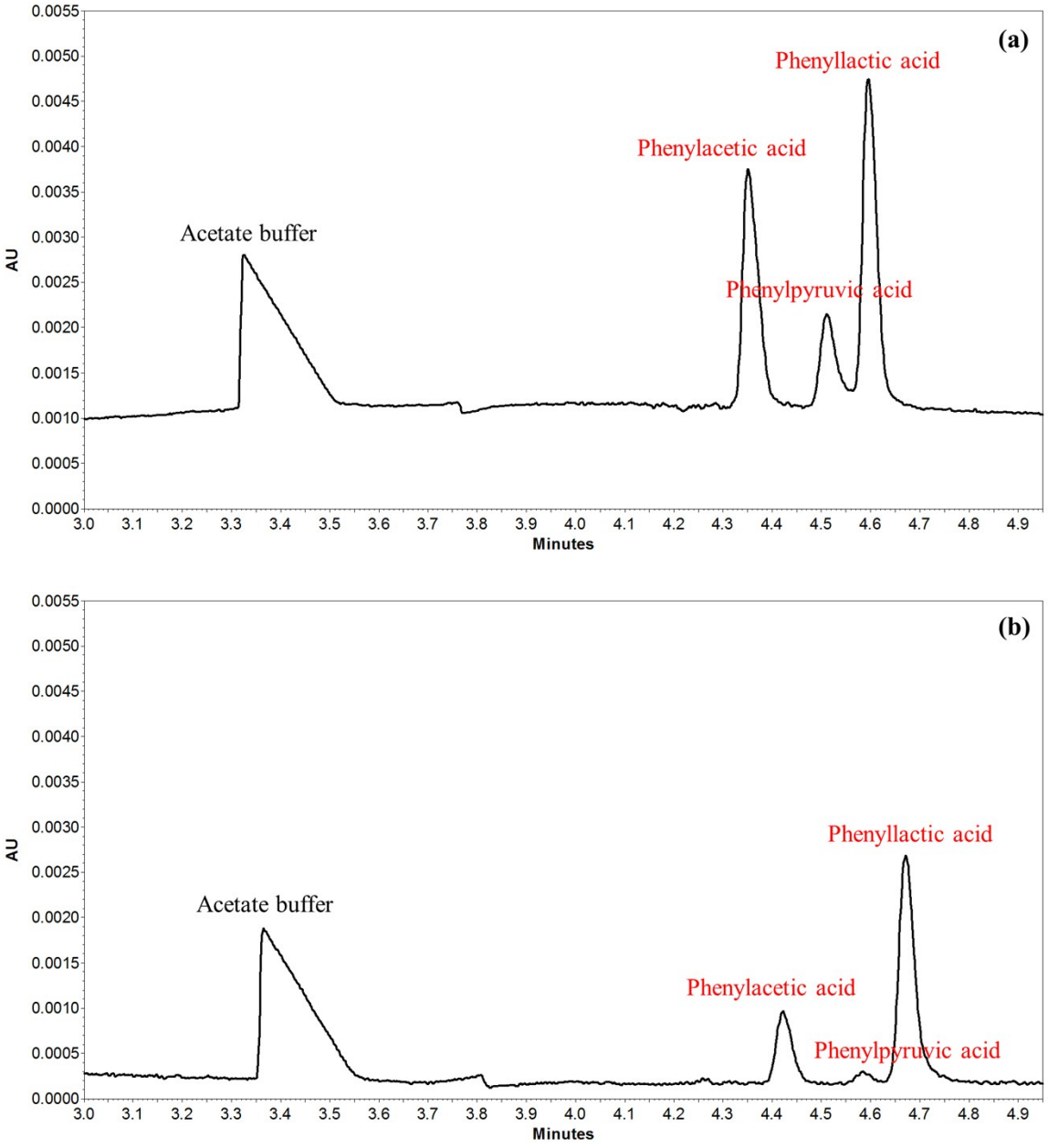

Figure S9. Illustrative electropherogram of (a) authentic organic substrates standard solution (30 µM phenylacetic acid, 20 µM phenylpyruvic acid, and 40 µM phenyllactic acid) and (b) filtered reaction solution collected 8 hours after addition of 500 M HMO to 50 µM phenyllactic acid. All solutions contain 5 mM acetate buffer (pH 4.0) and 10 mM NaCl.

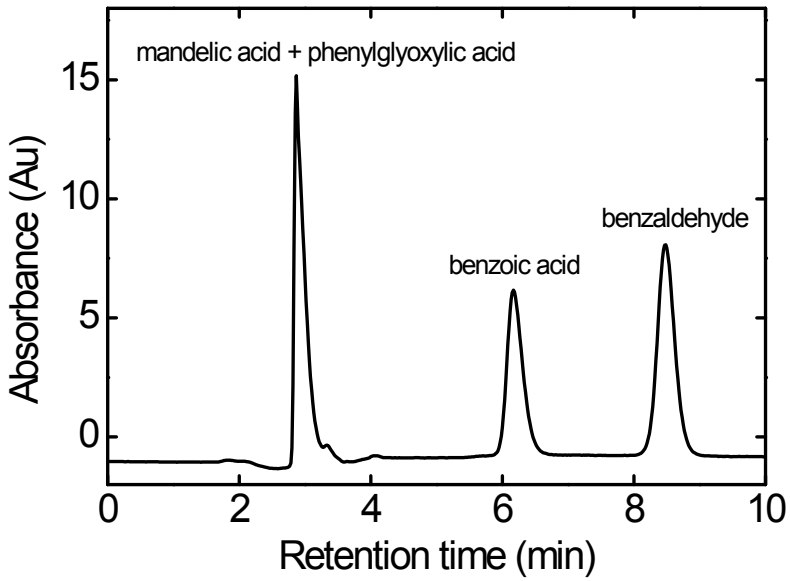

Figure S10. Illustrative HPLC chromatogram for a solution containing mandelic acid (40 μM), phenylglyoxylic acid (30 μM), benzoic acid (30 μM), benzaldehyde (40 μM).

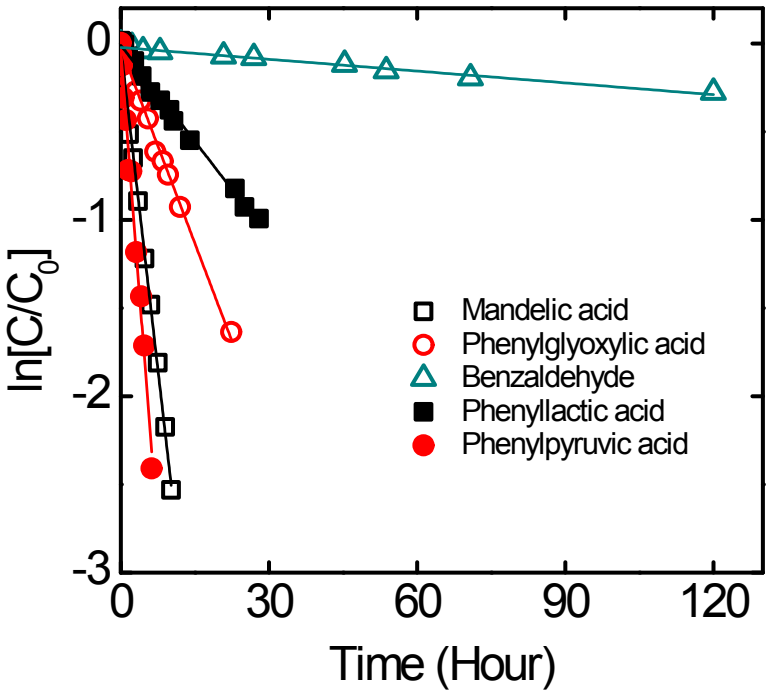

Organic substrate	Linear regression equation	R^2
Mandelic acid	$y = -0.256x - 0.0022$	0.998
Phenylglyoxylic acid	$y = -0.737x - 0.028$	0.994
Benzaldehyde	$y = -0.00220x - 0.022$	0.990
Phenyllactic acid	$y = -0.363x - 0.010$	0.993
Phenylpyruvic acid	$y = -0.365x - 0.042$	0.991

Figure S11. Semi-log plots of organic substrate as a function of time, with slope and intercept found using linear regression. Reaction conditions: 50 μM organic substrate, 500 μM HMO 5 mM acetate buffer (pH 4.0), and 10 mM NaCl.

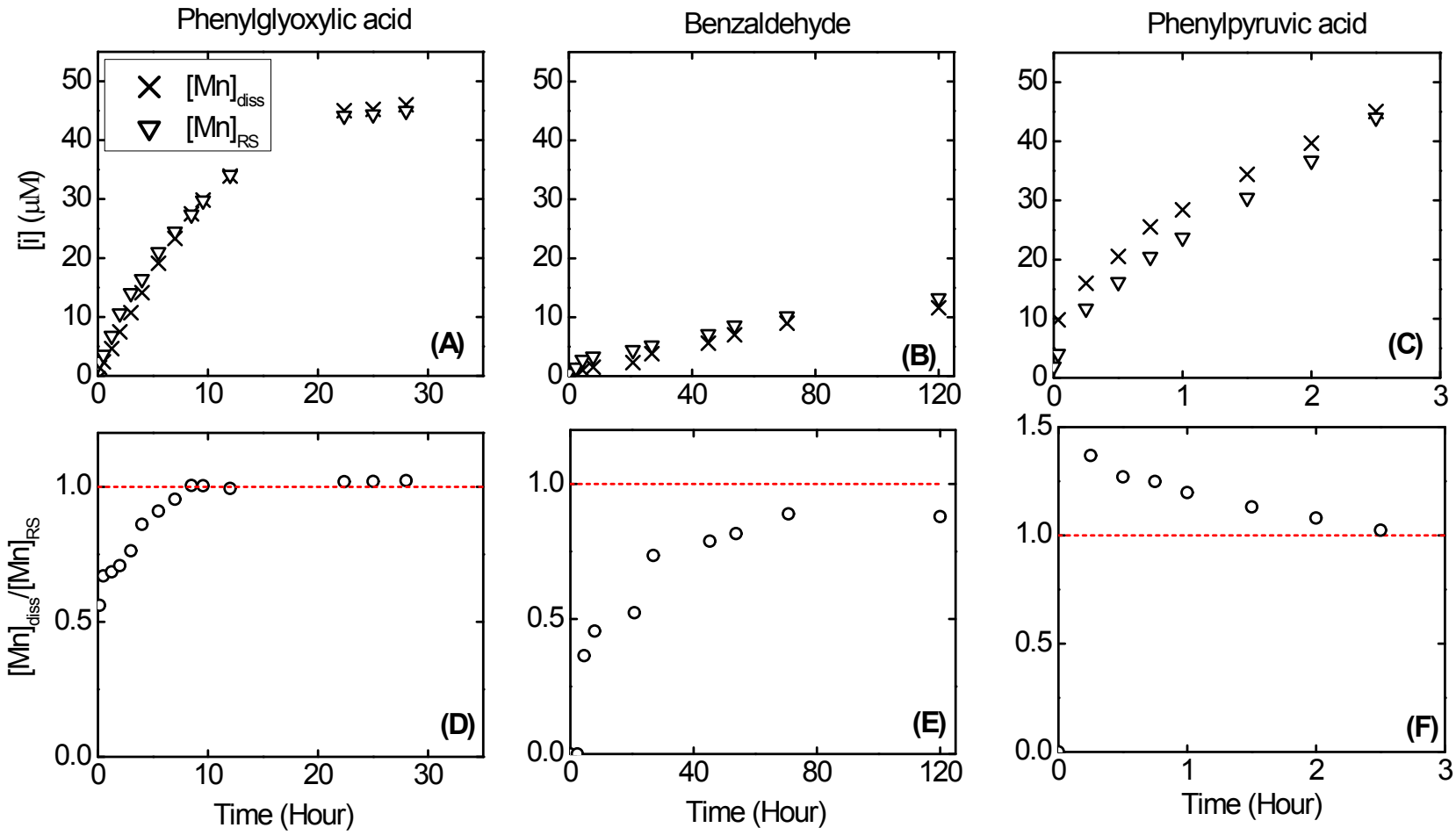

Figure S12. Using reaction stoichiometry to evaluate the oxidation of 50 μM phenylglyoxylic acid (A, D), benzaldehyde (B, E), or phenylpyruvic acid (C, F) by 500 μM HMO. Upper plots: $[Mn]_{diss}$ (×) refers to dissolved Mn measured by filtration and AAS. $[Mn]_{RS}$ (▽) is calculated from measurements of reaction set organic compounds, and expected reaction stoichiometries as discussed in the text. Lower plots: $[Mn]_{diss}/[Mn]_{RS}$ as a function of time. Reaction conditions: 5 mM acetate buffer (pH 4.0), and 10 mM NaCl.

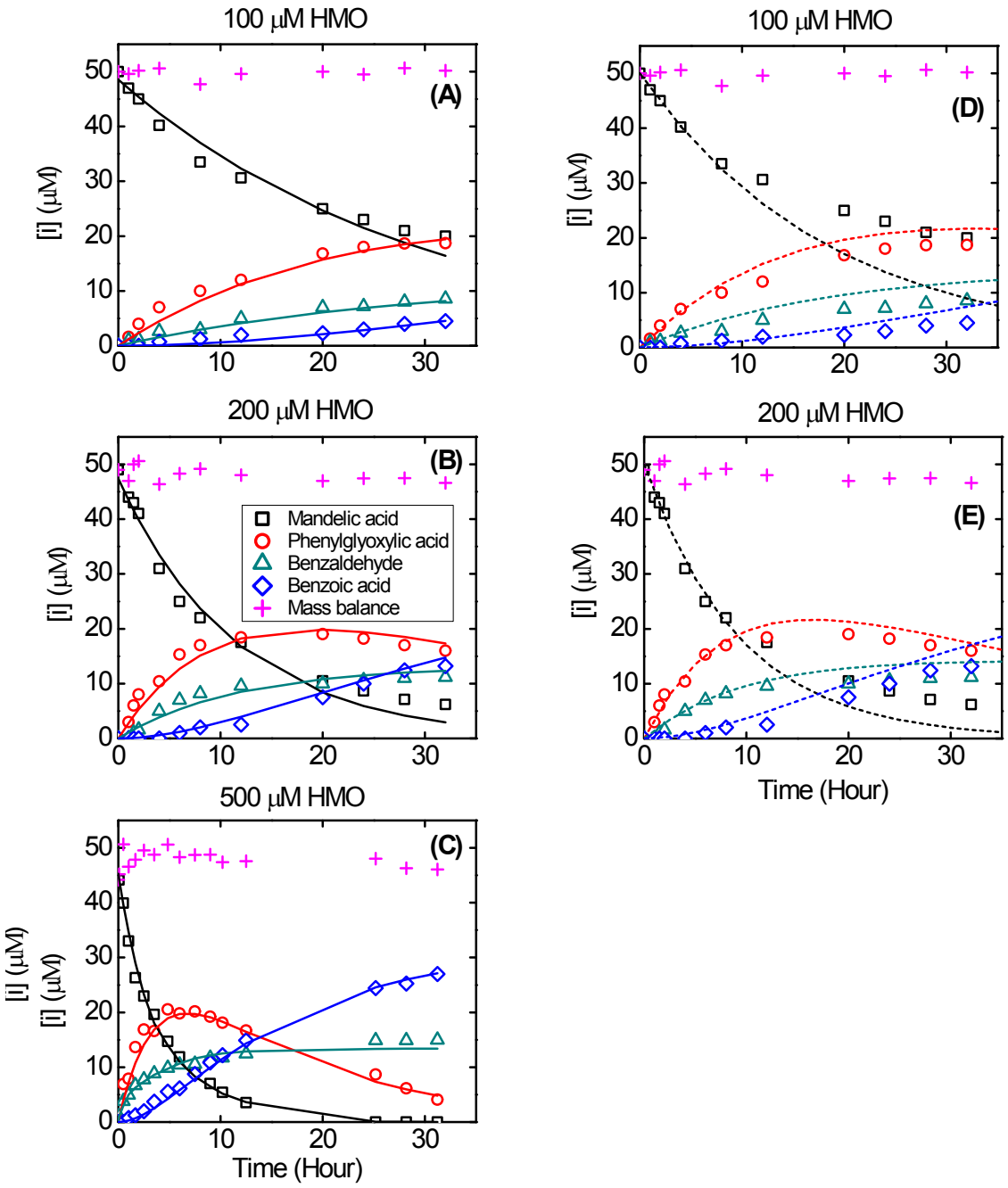

Figure S13. Oxidation of 50 μM mandelic acid by various loadings of HMO. Symbols represent measured organic substrates. Lines represent results from SCIENTIST numerical modeling. Left: Fitting parameters were obtained from the data set being shown. Right: fitting parameters from the 500 μM data set are applied to data obtained at 100 and 200 μM HMO data. Reaction conditions: 5 mM acetate buffer (pH 4.0), and 10 mM NaCl.

Scheme I: Hydrogen atom transfer

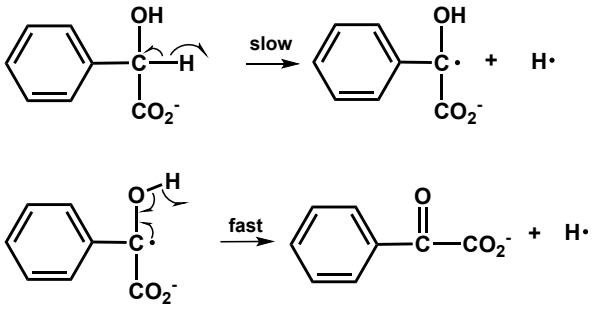

Scheme II: Hydride ion transfer

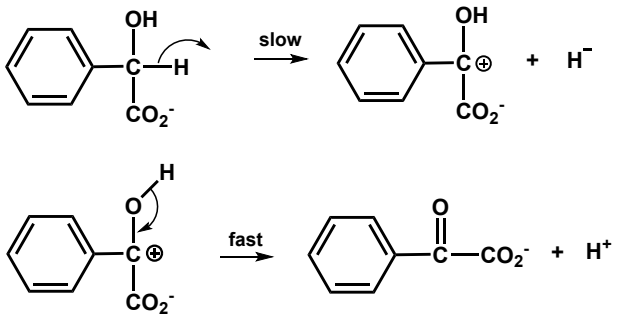

Figure S14. Reaction mechanisms of mandelic acid oxidation.

Keto acid hydration

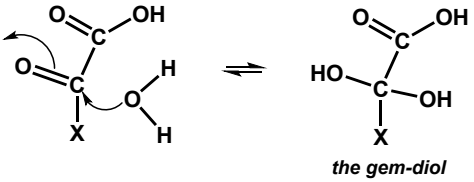

Aldehyde hydration

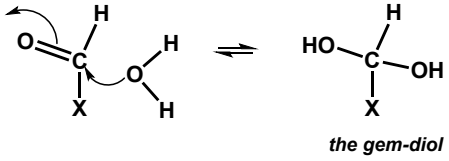

Keto acid tautomerization

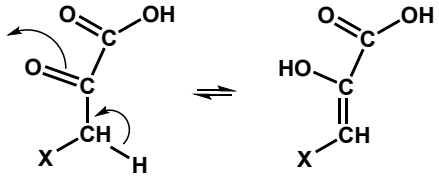

Figure S15. Electron pushing for keto acid and aldehyde hydration, and keto acid tautermerization.

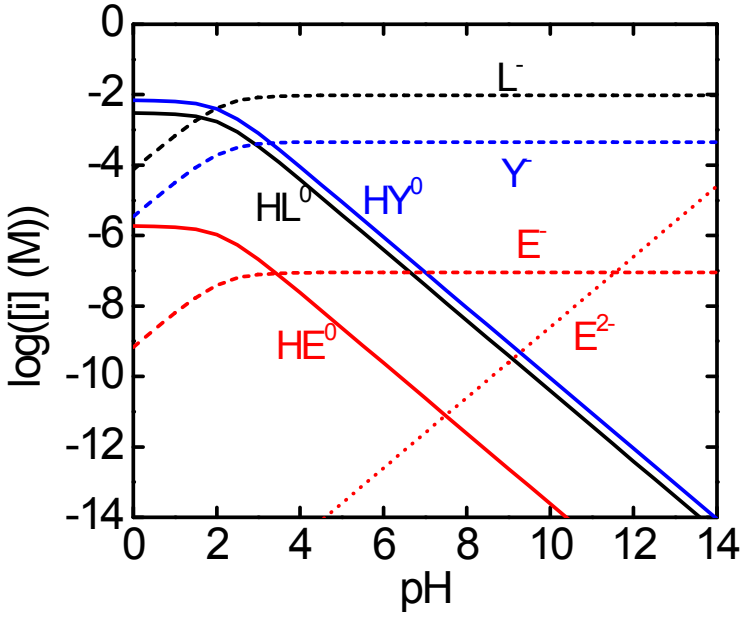

Figure S16. Equilibrium speciation of 10 mM pyruvic acid as a function of pH, based upon equilibrium constants provided in S3.

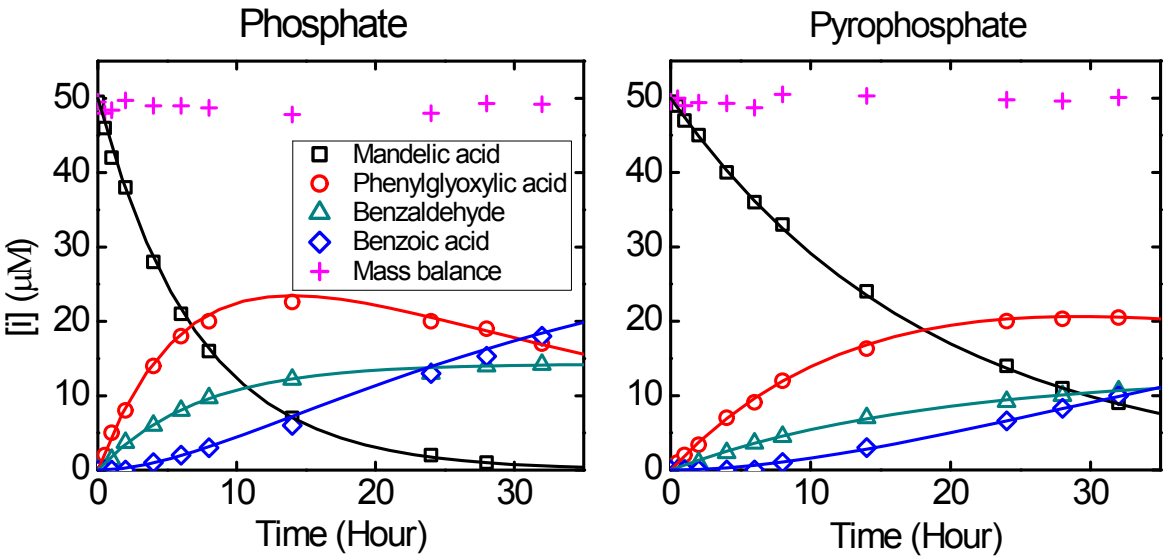

Figure S17. Effects of adding 500 μM phosphate and 500 μM pyrophosphate on oxidation of 50 μM mandelic acid by 500 μM HMO. Symbols represent measured organic substrates. Lines represent results from SCIENTIST numerical modeling. Reaction conditions: 5 mM acetate buffer (pH 4.0), and 10 mM NaCl.

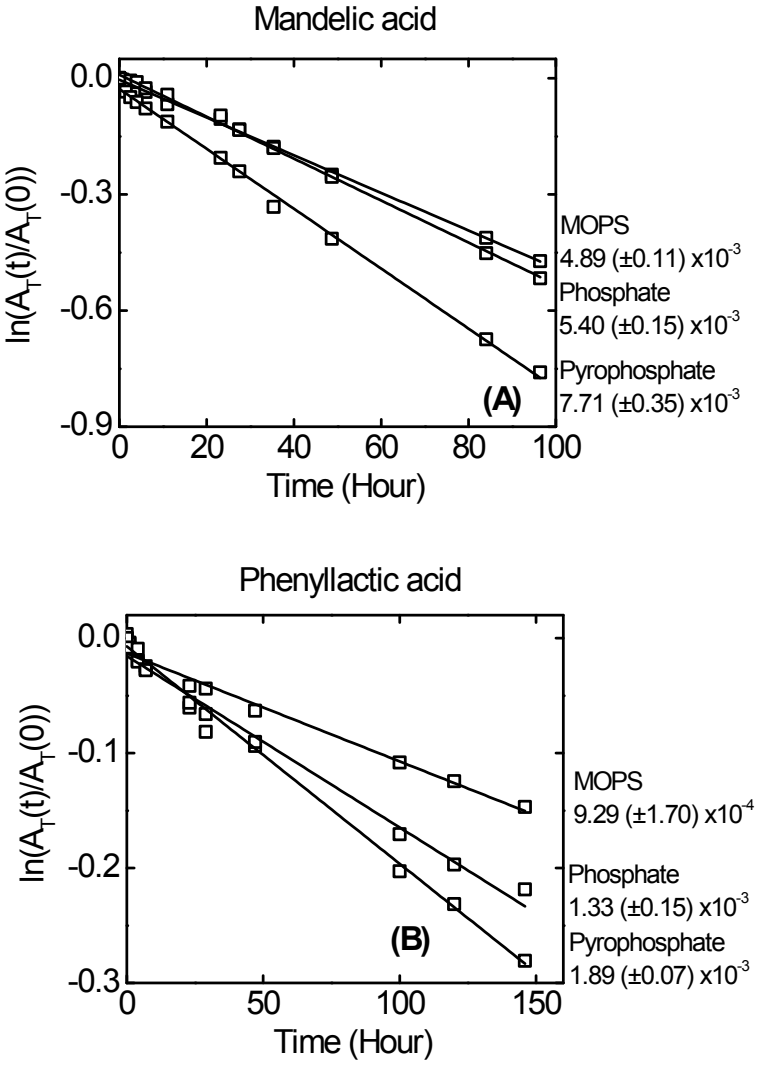

Figure S18. pH 7.0 experiments. Oxidation of 50 μM hydroxy acid by 500 μM HMO in medium employing 2.0 mM MOPS, phosphate, and pyrophosphate buffer. Semi-log plots for (A) mandelic acid and (B) phenyllactic acid loss. The ionic strength of the medium was maintained at 15 mM by NaCl.

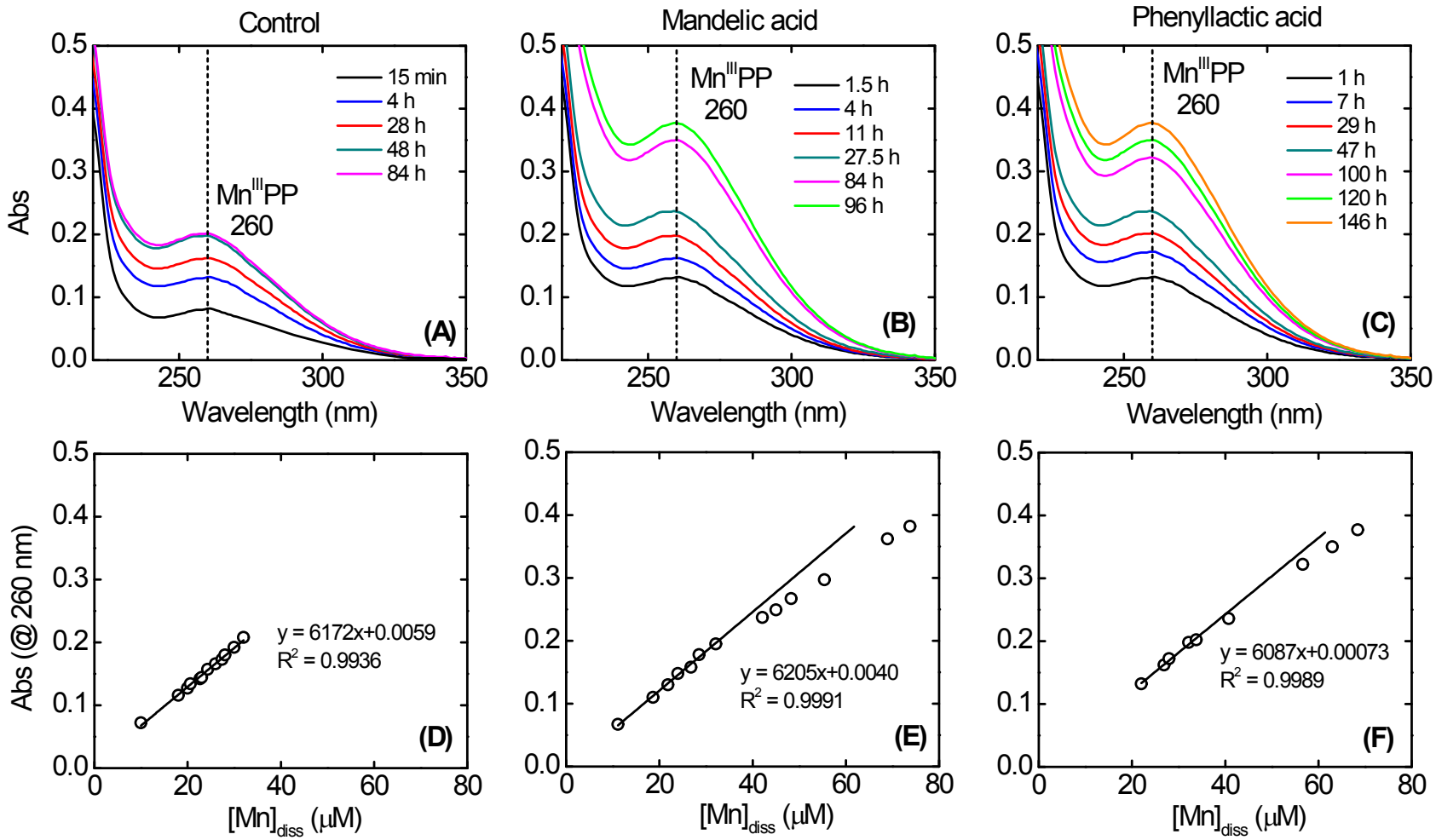

Figure S19. pH 7.0 experiments employing 2 mM pyrophosphate buffer. (A-C) Absorption spectra obtained by filtering organic substrate-free suspensions and mandelic acid- and phenyllactic acid-containing suspensions, with a similar peak at 260 nm, attributable to Mn^{III}-pyrophosphate complexes ($Mn^{III}PP$). (D-F) Absorbance at 260 nm as a function of dissolved Mn. Reactions were performed in substrate-free suspension or in suspensions containing 50 μM mandelic acid or phenyllactic acid. Suspensions contained 500 μM HMO. An ionic strength of 15 mM was fixed using NaCl addition.

References

1. A. Kornhauser, S. G. Coelho and V. J. Hearing, Applications of hydroxy acids: classification, mechanisms, and photoactivity, *Clin., Cosmet. Invest. Dermatol.*, 2010, **3**, 135-142.
2. R. J. Yu and E. J. V. Scott, Alpha-hydroxyacids and carboxylic acids, *J. Cosmet. Dermatol.*, 2004, **3**, 76-87.
3. T. Bond, E. H. Goslan, S. A. Parsons and B. Jefferson, A critical review of trihalomethane and haloacetic acid formation from natural organic matter surrogates, *Environ. Technol. Rev.*, 2012, **1**, 93-103.
4. R. A. Larson and A. L. Rockwell, Chloroform and chlorophenol production by decarboxylation of natural acids during aqueous chlorination, *Environ. Sci. Technol.*, 1979, **13**, 325-329.
5. J. Delaat, N. Merlet and M. Dore, Chlorination of organic compounds: chlorine demand and reactivity in relationship to the trihalomethane formation. Incidence of ammoniacal nitrogen, *Water Res.*, 1982, **16**, 1437-1450.
6. E. R. V. Dickenson, R. S. Summers, J. P. Croue and H. Gallard, Haloacetic acid and trihalomethane formation from the chlorination and bromination of aliphatic β-dicarbonyl acid model compounds, *Environ. Sci. Technol.*, 2008, **42**, 3226-3233.
7. S. Navalon, M. Alvaro and H. Garcia, Carbohydrates as trihalomethanes precursors. Influence of pH and the presence of Cl- and Br- on trihalomethane formation potential, *Water Res.*, 2008, **42**, 3990-4000.
8. D. S. Schechter and P. C. Singer, Formation of aldehydes during ozonation, *Ozone-Sci Eng*, 1995, **17**, 53-69.
9. J. Nawrocki, J. Swietlik, U. Raczyk-Stanislawiak, A. Dabrowska, S. Bilozor and W. Ilecki, Influence of ozonation conditions on aldehyde and carboxylic acid formation, *Ozone: Sci. Eng.*, 2003, **25**, 53-62.
10. X. Zhong, C. W. Cui and S. L. Yu, Identification of oxidation intermediates in humic acid oxidation, *Ozone: Sci. Eng.*, 2018, **40**, 93-104.
11. B. M. Tebo, J. R. Bargar, B. G. Clement, G. J. Dick, K. J. Murray, D. Parker, R. Verity and S. M. Webb, Biogenic manganese oxides: properties and mechanisms of formation, *Annu. Rev. Earth Planet. Sci.*, 2004, **32**, 287-328.
12. W. Boerjan, J. Ralph and M. Baucher, Lignin biosynthesis, *Annu. Rev. Plant Biol.*, 2003, **54**, 519-546.
13. M. Ragnar, C. T. Lindgren and N. O. Nilvebrant, pK_a-values of guaiacyl and syringyl phenols related to lignin, *J. Wood Chem. Technol.*, 2000, **20**, 277-305.
14. L. Pollegioni, F. Tonin and E. Rosini, Lignin-degrading enzymes, *FEBS J.*, 2015, **282**, 1190-1213.
15. C. N. Njiojob, J. L. Rhinehart, J. J. Bozell and B. K. Long, Synthesis of enantiomerically pure lignin dimer models for catalytic selectivity studies, *J. Org. Chem.*, 2015, **80**, 1771-1780.
16. C. Chen, H. Chang and T. K. Kirk, Aromatic-acids produced during degradation of lignin in spruce wood by *Phanerochaete-Chrysosporium*, *Holzforschung*, 1982, **36**, 3-9.
17. F. Berthold, C. T. Lindgren and M. E. Lindstrom, Formation of (4-hydroxy-3-methoxyphenyl)-glyoxylic acid and (4-hydroxy-3,5-dimethoxyphenyl)-glyoxylic acid

during polysulfide treatment of softwood and hardwood, *Holzforschung*, 1998, **52**, 197-199.
18. E. Baciocchi, M. F. Gerini, O. Lanzalunga and S. Mancinelli, Lignin peroxidase catalysed oxidation of 4-methoxymandelic acid. The role of mediator structure, *Tetrahedron*, 2002, **58**, 8087-8093.
19. R. Franke, I. Briesen, T. Wojciechowski, A. Faust, A. Yephremov, C. Nawrath and L. Schreiber, Apoplastic polyesters in *Arabidopsis* surface tissues - a typical suberin and a particular cutin, *Phytochemistry*, 2005, **66**, 2643-2658.
20. A. Otto, C. Shunthirasingham and M. J. Simpson, A comparison of plant and microbial biomarkers in grassland soils from the Prairie Ecozone of Canada, *Org. Geochem.*, 2005, **36**, 425-448.
21. Y. Sugiura, H. Tanaka, Y. Mino, T. Ishida, N. Ota, M. Inoue, K. Nomoto, H. Yoshioka and T. Takemoto, Structure, properties, and transport mechanism of iron(III) complex of mugineic acid, a possible phytosiderophore, *J. Am. Chem. Soc.*, 1981, **103**, 6979-6982.
22. D. Risse, H. Beiderbeck, K. Taraz, H. Budzikiewicz and D. Gustine, Corrugatin, a lipopeptide siderophore from *Pseudomonas corrugata. Z. Naturforsch*, 1998, **53C**, 295-304.
23. N. Ae, J. Arihara, K. Okada, T. Yoshihara and C. Johansen, Phosphorus uptake by pigeon pea and its role in cropping systems of the indian subcontinent, *Science*, 1990, **248**, 477-480.
24. J. D. Willey, M. T. Inscore, R. J. Kieber and S. A. Skrabal, Manganese in coastal rainwater: speciation, photochemistry and deposition to seawater, *J. Atmos. Chem.*, 2009, **62**, 31-43.
25. R. L. Siefert, A. M. Johansen, M. R. Hoffmann and S. O. Pehkonen, Measurements of trace metal (Fe, Cu, Mn, Cr) oxidation states in fog and stratus clouds, *J. Air Waste Manage. Assoc.*, 1998, **48**, 128-143.
26. J. G. Charrier and C. Anastasio, On dithiothreitol (DTT) as a measure of oxidative potential for ambient particles: evidence for the importance of soluble transition metals, *Atmos. Chem. Phys.*, 2012, **12**, 9321-9333.
27. Y. Lyu, H. B. Guo, T. T. Cheng and X. Li, Particle size distributions of oxidative potential of lung-deposited particles: assessing contributions from quinones and water-soluble metals, *Environ. Sci. Technol.*, 2018, **52**, 6592-6600.
28. K. Kawamura, R. Semere, Y. Imai, Y. Fujii and M. Hayashi, Water soluble dicarboxylic acids and related compounds in Antarctic aerosols, *J. Geophys. Res.: Atmos.*, 1996, **101**, 18721-18728.
29. P. Fu, K. Kawamura, K. Usukura and K. Miura, Dicarboxylic acids, ketocarboxylic acids and glyoxal in the marine aerosols collected during a round-the-world cruise, *Mar. Chem.*, 2013, **148**, 22-32.
30. M. Claeys, B. Graham, G. Vas, W. Wang, R. Vermeylen, V. Pashynska, J. Cafmeyer, P. Guyon, M. O. Andreae, P. Artaxo and W. Maenhaut, Formation of secondary organic aerosols through photooxidation of isoprene, *Science*, 2004, **303**, 1173-1176.
31. M. Claeys, R. Szmigielski, I. Kourtchev, P. Van der Veken, R. Vermeylen, W. Maenhaut, M. Jaoui, T. E. Kleindienst, M. Lewandowski, J. H. Offenberg and E. O. Edney, Hydroxydicarboxylic acids: Markers for secondary organic aerosol from the photooxidation of α-pinene, *Environ. Sci. Technol.*, 2007, **41**, 1628-1634.

32. R. J. Rapf, M. R. Dooley, K. Kappes, R. J. Perkins and V. Vaida, pH Dependence of the aqueous photochemistry of α-keto acids, *J. Phys. Chem. A*, 2017, **121**, 8368-8379.
33. M. Frosch, A. A. Zardini, S. M. Platt, L. Muller, M. C. Reinnig, T. Hoffmann and M. Bilde, Thermodynamic properties and cloud droplet activation of a series of oxo-acids, *Atmos. Chem. Phys.*, 2010, **10**, 5873-5890.
34. L. Schone and H. Herrmann, Kinetic measurements of the reactivity of hydrogen peroxide and ozone towards small atmospherically relevant aldehydes, ketones and organic acids in aqueous solutions, *Atmos. Chem. Phys.*, 2014, **14**, 4503-4514.
35. A. E. Martell, R. M. Smith and R. J. Motekaitis, *NIST Critically Selected Stability Constants of Metal Complexes, Version 8.0*, U.S. Department of Commerce, Washington, DC, 2004.
36. A. Lopalco, J. Douglas, N. Denora and V. J. Stella, Determination of pK_a and hydration constants for a series of α-keto-carboxylic acids using nuclear magnetic resonance spectrometry, *J. Pharm. Sci.*, 2016, **105**, 664-672.
37. W. J. Bover and P. Zuman, Lewis acid properties of benzaldehydes and substituent effects, *J. Chem. Soc., Perkin Trans. 2*, 1973, **6**, 786-790.
38. R. A. McClelland and M. Coe, Structure reactivity effects in the hydration of benzaldehydes, *J. Am. Chem. Soc.*, 1983, **105**, 2718-2725.
39. Y. Chiang, A. J. Kresge and P. Pruszynski, Keto-enol equilibria in the pyruvic acid system: determination of the keto enol equilibrium constants of pyruvic acid and pyruvate anion and the acidity constant of pyruvate enol in aqueous solution, *J. Am. Chem. Soc.*, 1992, **114**, 3103-3107.
40. R. C. Kerber and M. S. Fernando, α-Oxocarboxylic acids, *J. Chem. Educ.*, 2010, **87**, 1079-1084.
41. M. Galajda, T. Fodor, M. Purgel and I. Fabian, The kinetics and mechanism of the oxidation of pyruvate ion by hypochlorous acid, *Rsc Adv.*, 2015, **5**, 10512-10520.
42. Y. Chiang, A. J. Kresge, P. A. Walsh and Y. Yin, Phenylacetaldehyde and its *cis*- and *trans*-enols and enolate ions. Determination of the *cis:trans* ratio under equilibrium and kinetic control, *J. Chem. Soc., Chem. Commun.*, 1989, **13**, 869-871.